Korean J. Chem. Eng., **20**(1), 48-57 (2003)

Infrared and Raman Characterization of V_2O_5 on Zirconia Modified with WO_3 and Activity for Acid Catalysis

Jong Rack Sohn†, Jong Bae Park, Hae Won Kim* and Young Il Pae**

Dept. of Industrial Chemistry, Engineering College, Kyungpook National University, Daegu 702-701, Korea
*Dept. of Industrial Chemisry, Kyungil University, Kyungsan 712-701, Korea
**Dept. of Chemistry, University of Ulsan, Ulsan 680-749, Korea
(*Received 16 July 2002 • accepted 24 September 2002*)

Abstract−Vanadium oxide supported on zirconia modified with WO_3 was prepared by adding $Zr(OH)_4$ powder into a mixed aqueous solution of ammonium metavanadate and ammonium metatungstate followed by drying and calcining at high temperatures. The characterization of prepared catalysts was performed by using FTIR, Raman, and XRD. In the case of calcination temperature at 773 K, for samples containing low loading V_2O_5 below 18 wt%, vanadium oxide was in a highly dispersed state, while for samples containing high loading V_2O_5 equal to or above 18 wt%, vanadium oxide was well crystallized due to the high V_2O_5 loading on the surface of ZrO_2. The ZrV_2O_7 compound was formed through the reaction of V_2O_5 and ZrO_2 at 873 K, and the compound decomposed into V_2O_5 and ZrO_2 at 1,073 K, these results were confirmed by FTIR and XRD. Catalytic tests for 2-propanol dehydration and cumene dealkylation have shown that the addition of WO_3 to V_2O_5/ZrO_2 enhanced both catalytic activity and acidity of V_2O_5-WO_3/ZrO_2 catalysts. The variations in catalytic activities for both reactions are roughly correlated with the changes of acidity.

Key words: V_2O_5 on ZrO_2, FTIR and Raman, Acid Catalysis, 2-Propanol Dehydration, Cumene Dealkylation

INTRODUCTION

Vanadium oxides are widely used as catalysts in oxidation reactions, e.g., the oxidation of sulfur dioxide, carbon monoxide, and hydrocarbons [Miyata et al., 1989; Lakshmi et al., 1999; Sachtler, 1971]. These systems have also been found to be effective catalysts for the oxidation of methanol to methylformate [Busca et al., 1987] and for the selective catalytic reduction of nitrogen oxide [Armor, 1992; Alemany et al., 1995]. Much research has been done to understand the nature of active sites, the surface structure of catalysts as well as the role played by the promoter of the supported catalysts, using infrared (IR), X-ray diffraction (XRD), electron spin resonance (ESR) and Raman spectroscopy [Busca et al., 1987; Elmi et al., 1989; Miyata et al., 1987; Cavani et al., 1988]. So far, silica, titania, zirconia and alumina [Hatayama et al., 1991; Arco et al., 1990; Centi et al., 1991; Scharf et al., 1991; Sohn et al., 1996] have been commonly employed as the vanadium oxide supports.

Recently, metal oxides modified with sulfur compounds have been studied as strong solid acid catalysts [Ward and Ko, 1994; Kustov et al., 1994], especially sulfate promoted zirconia containing iron or manganese as promoters [Hsu et al., 1992; Wan et al., 1996] or noble metals to inhibit deactivation [Iglesia et al., 1993; Ebitani et al., 1991]. The high catalytic activity and small deactivation upon the addition of noble metals can be explained by both the elimination of coke by hydrogenation and hydrogenolysis [Vaudagna et al., 1997], and the formation of Brönsted acid sites from H_2 on the catalysts [Ebitani et al., 1991]. Recently, several workers reported zirconia-supported tungsten oxide as an alternative material in reactions requiring strong acid sites [Sohn and Bae, 2000; Barton et al., 1999; Scheithauer et al., 1998; Arata, 1990; Hino and Arata, 1987]. Several advantages of tungstate, over sulfate, as dopant include that it does not suffer from dopant loss during thermal treatment and it undergoes significantly less deactivation during catalytic reactions [Larsen et al., 1996]. However, comparatively few studies have been reported on binary oxide, vanadium oxide-tungsten oxide supported on zirconia. This paper describes Infrared and Raman characterization of V_2O_5 supported on zirconia and modified with WO_3, and catalytic activity for acid catalysis. For this purpose, the 2-propanol dehydration and cumene dealkylation are used as test reactions.

EXPERIMENTAL SECTION

1. Catalysts Preparation

Precipitate of $Zr(OH)_4$ was obtained by adding aqueous ammonia slowly into an aqueous solution of zirconium oxychloride (Aldrich) at room temperature with stirring until the pH of the mother liquor reached about 8. The precipitate thus obtained was washed thoroughly with distilled water until chloride ion was not detected by $AgNO_3$ solution, and was dried at room temperature for 12 h. The dried precipitate was powdered below 100 mesh.

Catalysts containing various vanadium oxide content and modified with WO_3 were prepared by adding $Zr(OH)_4$ powder into a mixed aqueous solution of ammonium metavanadate (NH_4VO_3) (Aldrich) and ammonium metatungstate [$(NH_4)_6(H_2W_{12}O_{40})\cdot nH_2O$] (Aldrich) followed by drying and calcining at high temperatures for 1.5 h. This series of catalysts were denoted by their weight percentage of V_2O_5 and WO_3 and calcination temperature. For example, $4V_2O_5$-$15WO_3/ZrO_2$(773) indicated the catalyst containing 4 wt% V_2O_5

†To whom correspondence should be addressed.
E-mail: jrsohn@knu.ac.kr
‡This paper is dedicated to Professor Baik-Hyon Ha on the occasion of his retirement from Hanyang University.

and 15 wt% WO_3 calcined at 773 K.

2. Procedure

2-Propanol dehydration was carried out at 433 and 453 K in a pulse microreactor connected to a gas chromatograph. Fresh catalyst in the reactor made of 1/4 in. stainless steel was pretreated at 673 K for 1 h in the nitrogen atmosphere. Pulses of 1 μl 2-propanol were injected into a N_2 gas stream which passed over 0.05 g of catalyst. Packing material for the gas chromatograph was Diethyleneglycol succinate on Shimalite and column temperature was 423 K. Catalytic activity for 2-propanol dehydration was represented as mole of propylene produced per gram of catalyst. Conversion was taken as the average of the first to sixth pulse values. Cumene dealkylation was carried out at 673-723 K in the same reactor as above. Packing material for the gas chromatograph was Benton 34 on chromosorb W and column temperature was 403 K. Catalytic activity for cumene dealkylation was represented as mole of benzene produced from cumene per gram of catalyst. Conversions for both reactions were taken as the average of the first to sixth pulse values.

FTIR absorption spectra of V_2O_5-WO_3/ZrO_2 powders were measured by KBr disk method over the range 1,200-400 cm^{-1}. The samples for the KBr disk method were prepared by grinding a mixture of the catalyst and KBr powders in an agate mortar and pressing them in the usual way, where the ratio of KBr to catalysts was 20. FTIR spectra of ammonia adsorbed on the catalyst were obtained in a heatable gas cell at room temperature with a Mattson Model GL 6030E spectrophotometer. The self-supporting catalyst wafers contained about 9 mg/cm^2. Prior to obtaining the spectra the samples were heated under vacuum at 673-773 K for 1.5 h.

The FT-Raman spectra were obtained with a Bruker model FRA 106 A spectrometer equipped with an InGaAs detector and a Nd : YAG laser source with a resolution of 4 cm^{-1}. The laser beam was focused onto an area 0.1×0.1 mm^2 in size of the sample surface; a 180° scattering geometry was used.

Catalysts were checked in order to determine the structure by means of a Joel Model JDX-8030 diffractometer, employing Cu$K\alpha$ (Ni-filtered) radiation. The specific surface area was determined by applying the BET method to the adsorption of N_2 at 77 K.

RESULTS AND DISCUSSION

1. Infrared and Raman Spectra

Fig. 1 shows IR spectra of V_2O_5-$15WO_3/ZrO_2$ (773) catalysts with various V_2O_5 contents calcined at 773 K for 1.5 h. Although with samples below 18 wt% of V_2O_5, definite peaks were not observed, the absorption bands at 1,022 and 820 cm^{-1} appeared for $18V_2O_5$-$15WO_3/ZrO_2$, $23V_2O_5$-$15WO_3/ZrO_2$, $28V_2O_5$-$15WO_3/ZrO_2$ and pure V_2O_5 containing high V_2O_5 content. The band at 1,022 cm^{-1} was assigned to the V=O stretching vibration, while that at 820 cm^{-1} was attributable to the coupled vibration between V=O and to V-O-V [Mori et al., 1987]. Generally, the IR band of V=O in crystalline V_2O_5 showed at 1,020-1,025 cm^{-1} and the Raman band at 995 cm^{-1} [Miyata et al., 1989; Bjorklund et al., 1989]. The decrease in crystallinity of V_2O_5, i.e., the formation of the amorphous phase for V_2O_5-WO_3/ZrO_2 of a low vanadium loading, is attributed to formation of the vanadate species dispersed on ZrO_2 in a monolayer; this results in the distortion of the structure, i.e., a weakening of the V=O bond.

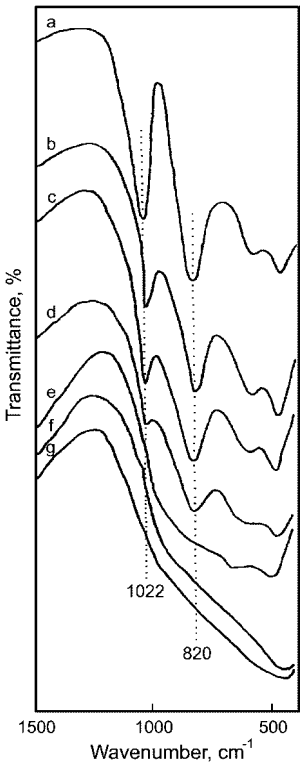

Fig. 1. Infrared spectra of catalysts calcined at 773 K: (a) V_2O_5, (b) $28V_2O_5$-$15WO_3/ZrO_2$, (c) $23V_2O_5$-$15WO_3/ZrO_2$, (d) $18V_2O_5$-$15WO_3/ZrO_2$, (e) $12V_2O_5$-$15WO_3/ZrO_2$, (f) $8V_2O_5$-$15WO_3/ZrO_2$, and (g) $4V_2O_5$-$15WO_3/ZrO_2$.

Consequently, the distorted structure brings about a shift of the band due to the V=O stretching vibration from 1,022 cm^{-1} to lower wave number [Miyata et al., 1987]. Roozeboom et al. [Roozeboom et al., 1980] have investigated the V_2O_5 species supported on various supporters by Raman spectroscopy and temperature-programmed reduction; they concluded that the band at 970 cm^{-1} is due to surface vanadate species present as a two-dimensional monolayer.

The intensity of the V=O absorption gradually decreased with decreasing V_2O_5 content, although the band position did not change. As shown in Fig. 1, the catalysts at vanadia loadings below 18 wt% gave no absorption bands due to crystalline V_2O_5. This observation suggests that vanadium oxide below 18 wt% is in a highly dispersed state. It was reported that high V_2O_5 loading on the surface of ZrO_2 is well crystallized and observed in the spectra of IR and solid state ^{51}V NMR [Sohn et al., 1996].

As shown in Fig. 1, for $4V_2O_5$-$15WO_3/ZrO_2$ and $12V_2O_5$-$15WO_3/ZrO_2$ calcined at 773 K the crystalline V_2O_5 was not observed in their IR spectra, suggesting the high dispersion of V_2O_5 on the surface of zirconia as the amorphous phase. However, it is necessary to examine the formation of crystalline V_2O_5 as a function of calcination temperature. Variation of IR spectra against calcination temperature for $4V_2O_5$-$15WO_3/ZrO_2$ is shown in Fig. 2. There were no V=O stretching bands at 1,022 cm^{-1} from 673 to 973 K of the calcination temperature, indicating no formation of crystalline V_2O_5. However, as shown in Fig. 2, V=O stretching bands due to crystalline V_2O_5 at 1,073 and 1,173 K appeared at 1,022 cm^{-1} together with lattice vibration bands of V_2O_5 and WO_3 below 900 cm^{-1} [Park et al., 2000; Highfield and Moffat, 1984]. The formation of crystal-

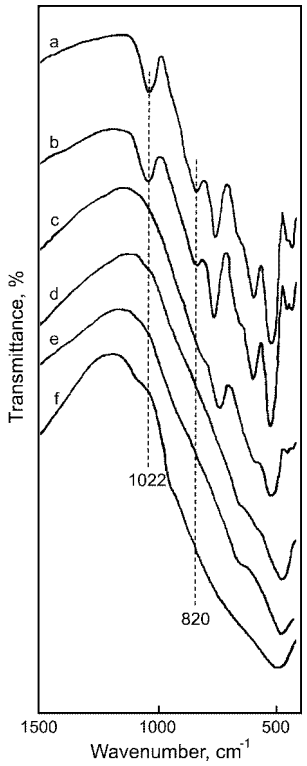

Fig. 2. Infrared spectra of $4V_2O_5$-$15WO_3/ZrO_2$ calcined at (a) 1,173 K, (b) 1,073 K, (c) 973 K, (d) 873 K, (e) 773 K, and (f) 673 K.

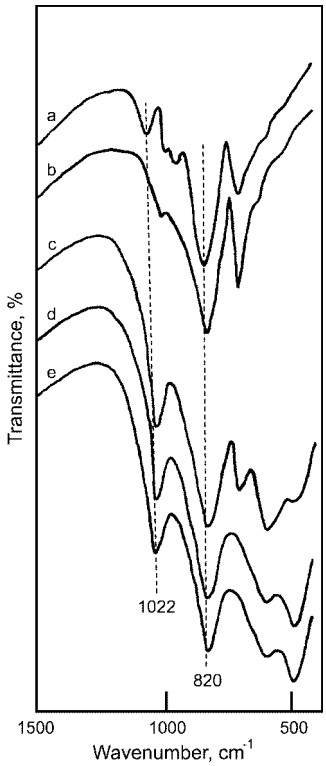

Fig. 3. Infrared spectra of $28V_2O_5$-$15WO_3/ZrO_2$ calcined at (a) 1,073 K, (b) 973 K, (c) 873 K, (d) 773 K, and (e) 673 K.

line V_2O_5 at above 1,073 K can be explained in terms of the decomposition of ZrV_2O_7 compound which was formed through the reaction of V_2O_5 and ZrO_2 at 873-973 K. In this study, on X-ray diffraction patterns described later, the cubic phase of ZrV_2O_7 was observed in the samples calcined at 873 K and for sample calcined at 1,173 K the ZrV_2O_7 phase disappeared due to the decomposition of ZrV_2O_7, leaving the V_2O_5 phase and the monoclinic phase of ZrO_2. In fact, it is known that the formation of ZrV_2O_7 from V_2O_5 and ZrO_2 occurs at 873 K of calcination temperature and the ZrV_2O_7 decomposes into ZrO_2 and V_2O_5 at 1,073 K [Sohn et al., 1996; Roozeboom et al., 1980]. In separate experiments, variation of IR spectra against calcination temperature for $12V_2O_5$-$15WO_3/ZrO_2$ (not shown in the Figure) was similar to that for $4V_2O_5$-$15WO_3/ZrO_2$ as shown in Fig. 2.

Fig. 3 shows IR spectra of $28V_2O_5$-$15WO_3/ZrO_2$ catalysts calcined at 673-1,073 K for 1.5 h. Unlike $4V_2O_5$-$15WO_3/ZrO_2$ and $12V_2O_5$-$15WO_3/ZrO_2$ catalysts, for $28V_2O_5$-$15WO_3/ZrO_2$ crystalline V_2O_5 appeared at a lower calcination temperature from 673 K to 873 K, and consequently V=O stretching band was observed at 1,022 cm^{-1}. This is because high V_2O_5 loading on the surface of ZrO_2 is well crystallized [Sohn et al., 1996]. However, at 973 K all V_2O_5 reacted with ZrO_2 and changed into ZrV_2O_7 so that V=O stretching at 1,022 cm^{-1} disappeared completely, as shown in Fig. 3. At 1,073 K of calcination temperature some of the ZrV_2O_7 decomposed into V_2O_5 and ZrO_2 and then V=O stretching band due to the crystalline V_2O_5 was again observed at 1,022 cm^{-1}.

Raman spectroscopy is a valuable tool for the characterization of dispersed metal oxides and detects vibrational modes of surface and bulk structures. In order to analyze the nature of the surface

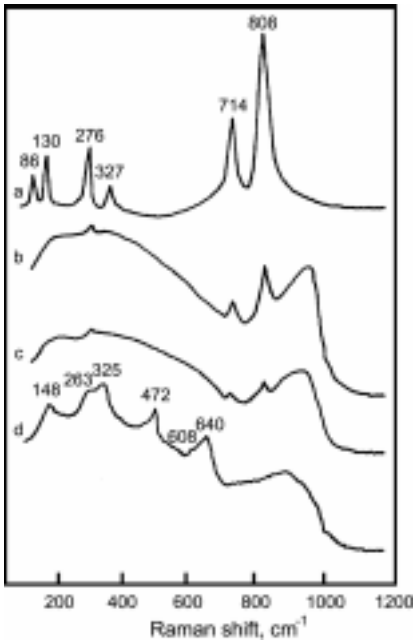

Fig. 4. Raman spectra of (a) WO_3, (b) $4V_2O_5$-$20WO_3/ZrO_2$ (773), (c) $4V_2O_5$-$10WO_3/ZrO_2$ (773), and (d) $4V_2O_5$-$5WO_3/ZrO_2$ (773).

species, laser Raman measurements of bulk WO_3 and V_2O_5-WO_3/ZrO_2 samples calcined at 773 K were made. Fig. 4 shows spectra of bulk WO_3 and $4V_2O_5$-WO_3/ZrO_2 (773) samples with different WO_3 loadings under ambient condition. The WO_3 structure is made up of distorted WO_3 octahedra. Bulk WO_3, obtained by calcining am-

monium metatungstate at 773 K, shows the main bands in good agreement with data previously reported [Salvati et al., 1981; Sohn and Park, 1998]. The major vibrational modes of WO_3 are located at 808, 714, and 276 cm^{-1}, and have been assigned to the W-O stretching mode, the W-O bending mode, and the W-O-W deformation mode, respectively [Chan et al., 1984]. Zhao et al. have observed the formation of WO_3 crystallines only when the monolayer capacity of WO_3 on zirconia has been exceeded [Zhao et al., 1996]. In this work the tungsten oxide exceeding the monolayer capacity of the zirconia support forms crystalline WO_3 under ambient conditions at elevated temperature. The crystalline WO_3 was also observed in the XRD patterns described below. So, as shown in Fig. 4(d), for $4V_2O_5$-$5WO_3/ZrO_2$ (773) no bands corresponding to WO_3 crystallites appear, indicating that WO_3 is in a highly dispersed state. In view of Fig. 4, a monolayer capacity for WO_3 seems to be between 5 and 10 wt%. As described in IR spectra, the catalysts at vanadia loadings below 18 wt% gave no absorption bands due to crystalline V_2O_5. As shown in Fig. 4, for the samples containing 4% V_2O_5 no bands due to V_2O_5 crystalline were observed, showing good agreement with the results of IR spectra.

The molecular structure of the supported tungsten oxide species depends on the loading. Several authors observed that the nature of surface tungsten species on Al_2O_3, TiO_2 and ZrO_2 depends on the amount of WO_3. For low tungsten loading there appear tetrahedrally coordinated tungsten oxide species; for high tungsten loading octahedral polymeric WO_3 species appear in addition to the tetrahedral ones [Sohn and Park, 1998; Engweiler et al., 1996; Vaudagna et al., 1998]. As shown in Fig. 4, at low tungsten loading tetrahedrally coordinated tungsten oxide species (at ~935 cm^{-1}) are predominantly formed, while with increased loading polytungstate species with an octahedral environment become predominant (at 965-985 cm^{-1}). The frequency of Raman features (1,000-940 cm^{-1}), the maximum of which shifts slightly upwards on increasing vanadium content, is assigned to the V=O stretching mode of vanadyl species in a hydrated form [Alemany et al., 1995; Ramis et al., 1990]. Therefore, the broad band observed in the 930-990 cm^{-1} region in Fig. 4 will be interpreted as an overlap of three characteristic bands (two tungsten oxide species and one vanadyl species). Tetragonal zirconia is expected to yield a spectrum consisting of six Raman bands with frequencies at about 148, 263, 325, 472, 608 and 640 cm^{-1}, while monoclinic zirconia exhibits the characteristic features at 180, 188, 221, 380, 476, and 637 cm^{-1} [Mercera et al., 1990; Scheithauer et al., 1998]. Therefore, as shown in Fig. 4(d), $4V_2O_5$-$5WO_3/ZrO_2$ sample exhibits the characteristic features of tetragonal zirconia, indicating no transformation of ZrO_2 from tetragonal to monoclinic. For high tungsten loading samples calcined at 773 K in Fig. 4(b and c), zirconia is amorphous to X-ray diffraction described below. The Raman spectrum of amorphous zirconia is characterized by a very weak and broad band at 550-600 cm^{-1} [Schild et al., 1991]. Therefore, the Raman band of amorphous zirconia in Figs. 4 and 5 is not well observed by overlapping of other bands.

We will discuss the Raman spectra of the series of V_2O_5-$15WO_3/ZrO_2$ (773) samples containing different V_2O_5 loadings, which are shown in Fig. 5. For both samples, $22V_2O_5$-$15WO_3/ZrO_2$ and $18V_2O_5$-$15WO_3/ZrO_2$ the spectra displayed bands at 144, 196, 284, 304, 406, 484, 528, 702 and 996 cm^{-1} all of which are characteristic of crystalline V_2O_5 [Dines et al., 1991]. These results are in good

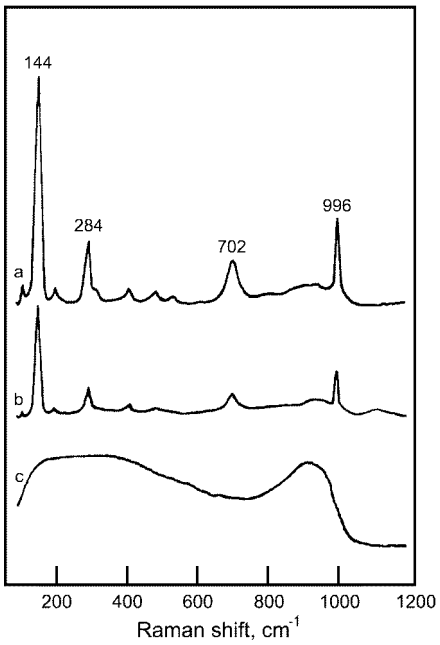

Fig. 5. Raman spectra of (a) $22V_2O_5$-$15WO_3/ZrO_2$ (773), (b) $18V_2O_5$-$15WO_3/ZrO_2$ (773), and (c) $8V_2O_5$-$15WO_3/ZrO_2$ (773).

agreement with those of the IR mentioned above. The 996 cm^{-1} band is assigned to the vibration of the short vanadium oxygen bond normally regarded as a V=O species [Dines et al., 1991]. However, for $8V_2O_5$-$15WO_3/ZrO_2$ containing low V_2O_5 loading, no bands due to crystalline V_2O_5 are observed, indicating high dispersion of V_2O_5 on the ZrO_2 surface. A broad band containing a maximum at 940 cm^{-1} is associated with the overlap of three characteristic bands by two tungsten oxide species and one vanadyl species discussed above.

The IR spectra in Figs. 1-3 have been taken in contact with air and KBr pressed disks. The Raman spectra in Figs. 4 and 5 have been taken in air by using the sample powders. To examine the structure of metal oxides supported on ZrO_2 under dehydration conditions, IR spectra of V_2O_5-WO_3/ZrO_2 samples (self-supporting wafers) were obtained in a heatable gas cell after evacuation at 773 K for 1.5 h. The IR spectra for $4V_2O_5$-$15WO_3/ZrO_2$ and $18V_2O_5$-$15WO_3/ZrO_2$(773) are presented for the range, 1,200-800 cm^{-1} in Fig. 6. For $4V_2O_5$-$15WO_3/ZrO_2$ and $18V_2O_5$-$15WO_3/ZrO_2$ samples, the IR band at 1,012 cm^{-1} after evacuation at 773 K is due to the W=O stretching mode of the tungsten oxide complex bonded to the ZrO_2 surface [Sohn and Park, 1998; Barton et al., 1999]. As shown in Fig. 6, these W=O bands due to wolframyl species only appear on evacuated samples, being undetectable on wet samples. This can be rationalized by assuming that the adsorption of water causes a strong perturbation of the corresponding tungsten oxide species, with a consequent strong broadening and shift down of these bands which become almost undetectable [Gutierrez-Alejandre et al., 1998]. The IR band at 1,012 cm^{-1} matches the Raman absorption at 1,015 cm^{-1} [Vuurman et al., 1991]. However, the band at 1,015 cm^{-1} in Figs. 4 and 5 was not observed because Raman spectra were recorded under ambient conditions. These isolated tungsten oxides species are stabilized through multiple W-O-Zr bonds between each tungsten oxide species and the zirconia surface [Scheithauer et al., 1998; Barton et al., 1999]. Zhao et al. observed, in the Raman spec-

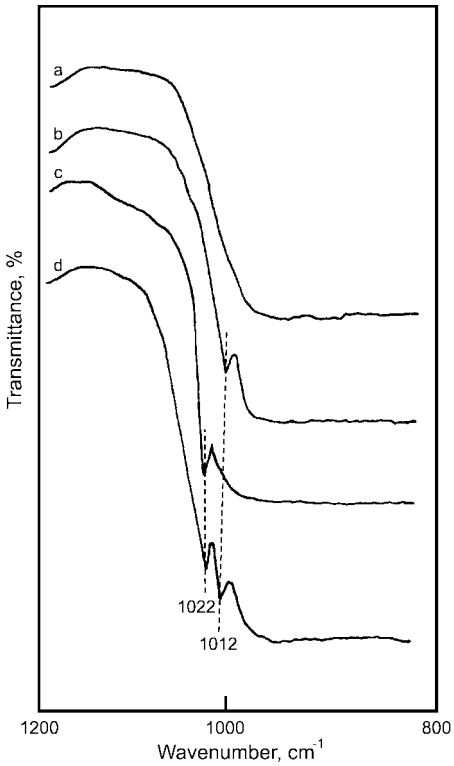

Fig. 6. IR spectra of $4V_2O_5$-$15WO_3/ZrO_2$ evacuated at (a) 298 K and (b) 773 K, and of $18V_2O_5$-$15WO_3/ZrO_2$ evacuated at (c) 298 K and (d) 773 K.

trum of WOx-ZrO_2, a band at 580 cm^{-1}, assigned to a W-O-Zr species [Zhao et al., 1996]. Upon dehydration at elevated temperature, the hydrated surface metal oxide species are unstable and decompose to form dehydrated surface metal oxide species by direct interaction with the surface OH groups of support, giving the formation of metal-oxygen-support bond [Kim et al., 1996].

For $18V_2O_5$-$15WO_3/ZrO_2$ sample the band at 1,022 cm^{-1} is due to the V=O stretching vibration of crystalline V_2O_5 as mentioned above, because V_2O_5 loading exceeding the formation of monolayer on the surface of ZrO_2 is well crystallized [Sohn et al., 1996]. Therefore, with $4V_2O_5$-$15WO_3/ZrO_2$ the definite peak due to the crystalline V_2O_5 is undetectable, explaining that vanadium oxide loading below 18 wt% is in a highly dispersed state.

2. Crystalline Structure of Catalyst

The crystalline structures of V_2O_5-WO_3/ZrO_2 calcined in air at different temperatures for 1.5 h were examined. For the $4V_2O_5$-$15WO_3/ZrO_2$, as shown in Fig. 7, ZrO_2 is amorphous to X-ray diffraction up to 673 K, with a tetragonal phase of ZrO_2 at 773-873 K, a two-phase mixture of the tetragonal and monoclinic ZrO_2 forms at 973 K, and a monoclinic phase of ZrO_2 at 1,073-1,173 K. Three crystal structures of ZrO_2, tetragonal, monoclinic and cubic phases have been reported [Larsen et al., 1997; Afansiev et al., 1994].

On the other hand, V_2O_5 for $4V_2O_5$-$15WO_3/ZrO_2$ and $12V_2O_5$-$15WO_3/ZrO_2$ is amorphous to X-ray diffraction up to 773 K, indicating that vanadium oxide is in a highly dispersed state and showing a good agreement with the results of IR in Fig. 1. In separate XRD experiments, the cubic phase of ZrV_2O_7 began to be observed in the sample of $12V_2O_5$-$15WO_3/ZrO_2$ calcined at 873 K and the

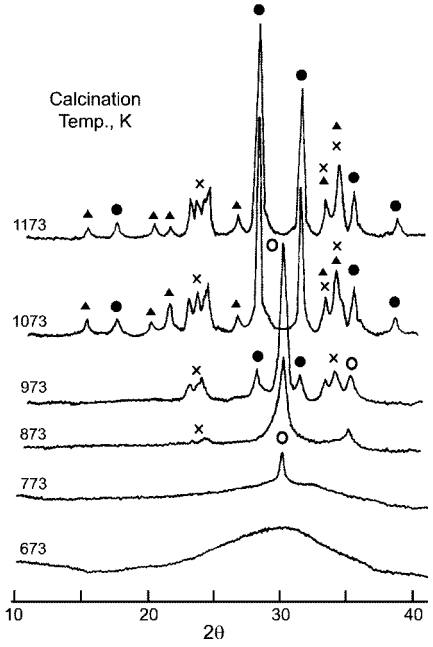

Fig. 7. X-ray diffraction patterns of $4V_2O_5$-$15WO_3/ZrO_2$ calcined at different temperatures. ○, tetragonal phase ZrO_2; ●, monoclinic phase ZrO_2; ▲, V_2O_5; ×, WO_3.

peak intensities of ZrV_2O_7 increased to some extent at 973 K (not shown in the Fig.). However, for samples calcined at 1,073-1,173 K the ZrV_2O_7 phase disappeared due to the complete decomposition of ZrV_2O_7 [Roozeboom et al., 1980], leaving only the crystalline V_2O_5 phase and the monoclinic phase of ZrO_2. The triclinic phase of crystalline WO_3 due to the decomposition of ammonium metatungstate was observed in the samples calined at 873-1,173 K.

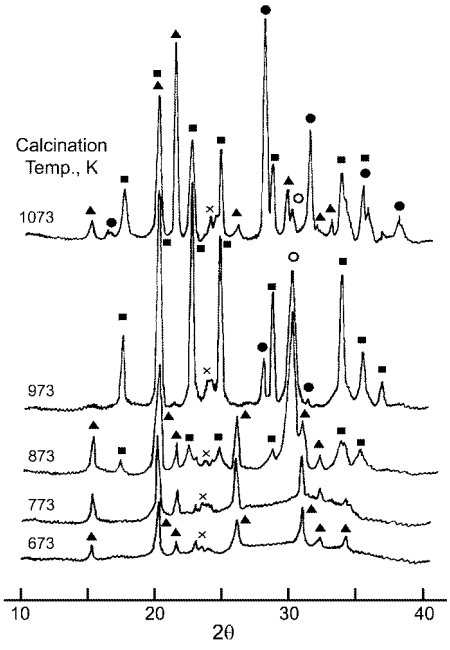

Fig. 8. X-ray diffraction patterns of $28V_2O_5$-$15WO_3/ZrO_2$ calcined at different temperatures. ○, tetragonal phase ZrO_2; ●, monoclinic phase ZrO_2; ▲, V_2O_5; ■, ZrV_2O_7; ×, WO_3.

However, as shown in Fig. 7, for the sample of $4V_2O_5$-$15WO_3$/ZrO_2 the crystalline ZrV_2O_7 on X-ray diffraction pattern was not observed at 873 K of calcination temperature. This indicates that for $4V_2O_5$-$15WO_3/ZrO_2$, the ZrV_2O_7 crystallites formed are less than 4 nm in size, that is, beyond the detection capability of the XRD technique [Sohn et al., 1996].

As shown in Fig. 8, in the case of $28V_2O_5$-$15WO_3/ZrO_2$ containing high content of V_2O_5 the crystalline V_2O_5 phase was observed even at 673 K of low calcination temperature, indicating that high V_2O_5 loading on the surface of ZrO_2 is well crystallized [Sohn et al., 1996]. These results are in good agreement with that of IR in Fig. 3 described above. From 873 K of calcination temperature V_2O_5 began to react with ZrO_2 to form ZrV_2O_7 compound and at 973 K the crystalline V_2O_5 phase disappeared completely, due to the consumption of V_2O_5 for the formation of ZrV_2O_7 compound. However, at 1,073 K, the crystalline V_2O_5 phase was observed again through the decomposition of ZrV_2O_7 compound [Sohn et al., 1996], as shown in Fig. 8. For $28V_2O_5$-$15WO_3/ZrO_2$ ZrO_2 was amorphous to X-ray diffraction up to 773 K, with a tetragonal phase of ZrO_2 at 873 K, and a two-phase mixture of the tetragonal and monoclinic forms at 973-1,073 K. From 673 K of calcination temperature the crystalline WO_3 phase was observed due to the decomposition of ammonium metatungstate.

3. Surface Properties

The specific surface areas of some samples calcined at 673 and 773 K for 1.5 h are listed in Table 1. The presence of vanadium oxide and tungsten oxide influences the surface area in comparison with the pure ZrO_2. Specific surface areas of V_2O_5-WO_3/ZrO_2 samples are larger than that of pure ZrO_2 calcined at the same temperature. It seems likely that the interaction between vanadium oxide (or tungsten oxide) and ZrO_2 protects catalysts from sintering [Sohn et al., 1996].

Infrared spectroscopic studies of ammonia adsorbed on solid surfaces have made it possible to distinguish between Brönsted and Lewis acid sites [Sohn et al., 2002; Larrubia et al., 2000]. The IR spectra of ammonia adsorbed on $4V_2O_5$-$15WO_3/ZrO_2$ calcined at 973 K and evacuated at 673 K for 1 h indicated the presence of both Brönsted and Lewis acid sites. Other samples having different vanadium content also showed the presence of both Lewis and Brönsted acids. Therefore, these V_2O_5-WO_3/ZrO_2 samples can be used as catalysts for Lewis or Brönsted acid catalysis.

Table 1. Specific surface areas of some V_2O_5-WO_3/ZrO_2 samples calcined at 673 K and 773 K

Catalysts	Surface area (m^2/g, 673 K)	Surface area (m^2/g, 773 K)
ZrO_2	185	122
$0.4V_2O_5$-$15WO_3/ZrO_2$	235	207
$1V_2O_5$-$15WO_3/ZrO_2$	239	211
$4V_2O_5$- $5WO_3/ZrO_2$	238	198
$4V_2O_5$-$10WO_3/ZrO_2$	246	212
$4V_2O_5$-$15WO_3/ZrO_2$	224	201
$4V_2O_5$-$20WO_3/ZrO_2$	218	196
$8V_2O_5$-$15WO_3/ZrO_2$	201	198
$12V_2O_5$-$15WO_3/ZrO_2$	217	188
$18V_2O_5$-$15WO_3/ZrO_2$	206	176
$20V_2O_5$-$15WO_3/ZrO_2$	171	149
$28V_2O_5$-$15WO_3/ZrO_2$	144	106

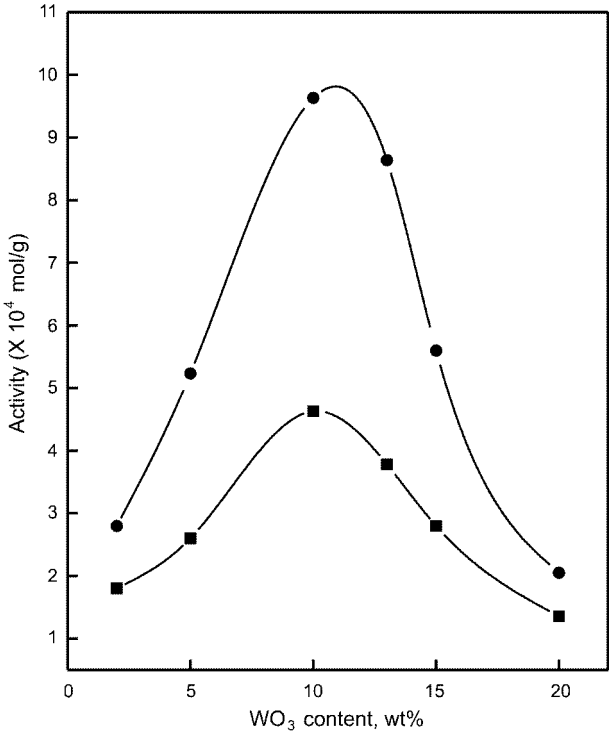

Fig. 9. Catalytic activity of $4V_2O_5$-WO_3/ZrO_2 (1023) for 2-propanol dehydration as a function of WO_3 content. ●, 453 K; ■, 433 K.

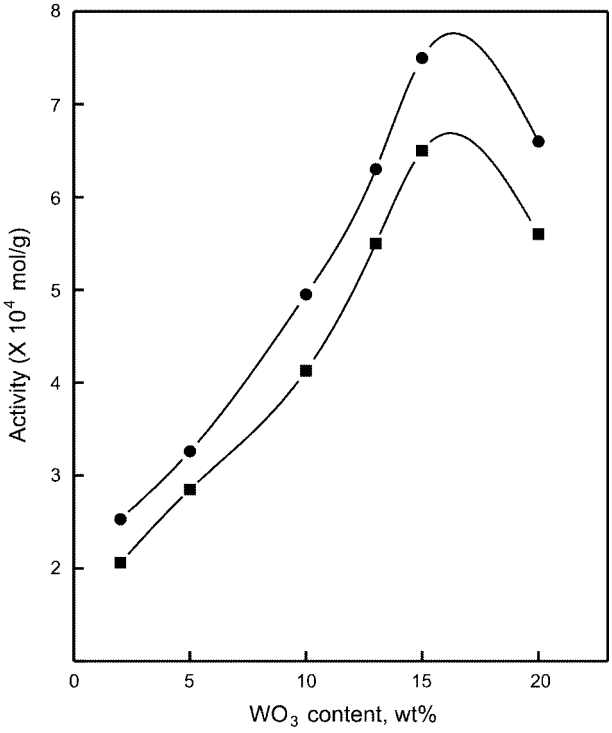

Fig. 10. Catalytic activity of $4V_2O_5$-WO_3/ZrO_2 (1023) for cumene dealkylation as a function of WO_3 content. ●, 723 K; ■, 673 K.

Table 2. Acidity of $4V_2O_5$-WO_3/ZrO_2 (1023) containing different WO_3 contents

Catalysts	Acidity (μmol/g)
$4V_2O_5$- $2WO_3/ZrO_2$	26.3
$4V_2O_5$-$5WO_3/ZrO_2$	31.7
$4V_2O_5$-$10WO_3/ZrO_2$	40.2
$4V_2O_5$-$13WO_3/ZrO_2$	27.1
$4V_2O_5$-$15WO_3/ZrO_2$	24.9
$4V_2O_5$-$20WO_3/ZrO_2$	18.8

4. Catalytic Activities for Acid Catalysis

It is also interesting to examine how the catalytic activity of an acid catalyst depends on its acidic properties [Lee and Rhee, 1997; Yuan et al., 2002]. The catalytic activities for the 2-propanol dehydration and cumene dealkylation are measured and the results are illustrated as a function of WO_3 content in Figs. 9 and 10, respectively. The addition of WO_3 to $4V_2O_5/ZrO_2$ up to 10-15 wt% caused the increases in the catalytic activities for both reactions. The increases of catalytic activities for both reactions are due to the increase of acidic sites. In separate experiments, the acidity of the catalysts, as determined by the amount of NH_3 irreversibly adsorbed at 503 K [Sohn et al., 1996; Sohn and Park, 1998], increased with the addition of WO_3 to $4V_2O_5/ZrO_2$, as listed in Table 2. In view of Table 2 and Figs. 9 and 10, the variations in catalytic activities for both reactions are roughly correlated with the changes of acidity. The differences of catalytic activities for both reactions against acidity are due to the difference of necessary acid strength for both reactions to occur. In fact, it has been known that 2-propanol dehydration takes place very readily on weak acid sites, while cumene dealkylation does on relatively strong acid sites [DeCanio et al., 1986]. In view of the catalytic data shown in Figs. 9 and 10 for 2-propanol dehydration and cumene dealkylation reactions, where the reaction temperatures were 433-453 K for the former and 673-723 K for the latter, it is clear that 2-propanol dehydration takes place more readily than cumene dealkylation. Recently, Toda et al. reported that the addition of WO_3 to V_2O_5 series catalysts led to an increase of the number of both Lewis and Brönsted acidic sites [Toda et al., 1999]. From the IR results of V=O bands they also reported that the majority of WO_3 incorporated onto the V_2O_5/ZrO_2 catalysts seems to be intercalated between vanadia and zirconia [Toda et al., 1999]. It has been also reported that for V_2O_5-WO_3/TiO_2 catalyst the electronic interaction between V and W oxides surface species may occur through oxygen bridging of the polyhedra and/or through the conduction band of TiO_2 [Alemony et al., 1995]. The former possibility is consistent with the formation of mixed WxVyOz species and with the detection of relatively isolated VO^{2+} ions that are slightly different from those monitored over V_2O_5/TiO_2 by EPR.

Considering the correlationship between acidity and catalytic activities for 2-propanol dehydration and cumene dealkylation, and the experimental results of other investigators [Alemony et al., 1995; Toda et al., 1999; Paganini et al., 1997], it is suggested that the increase of acidic sites and their strength may be attributable to electronic and structural interaction between vanadium oxide and tungsten oxide species on the ZrO_2 surface. Evidence for the existence of interaction between vanadium oxide and tungsten oxide species has also been provided by acidic catalytic tests for 2-propanol dehydration and cumene dealkylation. The catalytic tests for both reactions have shown that the addition of WO_3 to V_2O_5/ZrO_2 enhanced both catalytic activity (Figs. 9 and 10) and acidity of V_2O_5-WO_3/ZrO_2 catalysts.

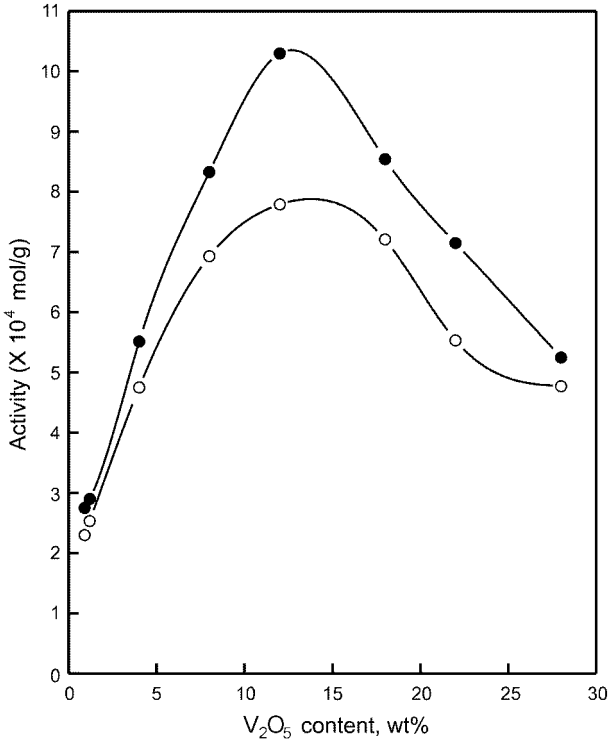

Fig. 11. Catalytic activity of V_2O_5-$15WO_3/ZrO_2$ (1023) for 2-propanol dehydration and cumene dealkylation as a function of V_2O_5 content. ●, 453 K for 2-propanol dehydration; ○, 673 K for cumene dealkylation.

The catalytic activities of V_2O_5-$15WO_3/ZrO_2$ for the 2-propanol dehydration and cumene dealkylation are measured and the results are illustrated as a function of V_2O_5 content in Fig. 11, where reaction temperatures are 453 K for the 2-propanol dehydration and 673 K for the cumene dealkylation. The catalytic activities for both reactions increased with the V_2O_5 content, giving maxima at 12% of V_2O_5, and then the activities decreased. We measured the acidity of V_2O_5-$15WO_3/ZrO_2$ as a function of V_2O_5 content. However, the variations in catalytic activities for both reactions were not correlated with the changes of acidity. Therefore, it is concluded that the increased catalytic activities up to 12% of V_2O_5 are not because of the increased acidity. This result may be attributed to the fact that for V_2O_5-$15WO_3/ZrO_2$ catalysts vanadium oxide up to 12 wt% is in a highly dispersed state or that the electronic interaction between V and W oxides species may occur through the intercalation of WO_3 between vanadia and zirconia [Toda et al., 1999; Alemony et al., 1995].

Catalytic activities of $4V_2O_5$-$10WO_3/ZrO_2$ are plotted as a function of calcinations temperature for 2-propanol dehydration in Fig. 12. The activities increased with the calcination temperature, giving a maximum at 973 K and then the activities decreased. Catalytic activities of $12V_2O_5$-$15WO_3/ZrO_2$ for cumene dealkylation are also plotted as a function of calcination temperature in Fig. 13. The activities also exhibited a maximum at 1,023 K. The decrease of activi-

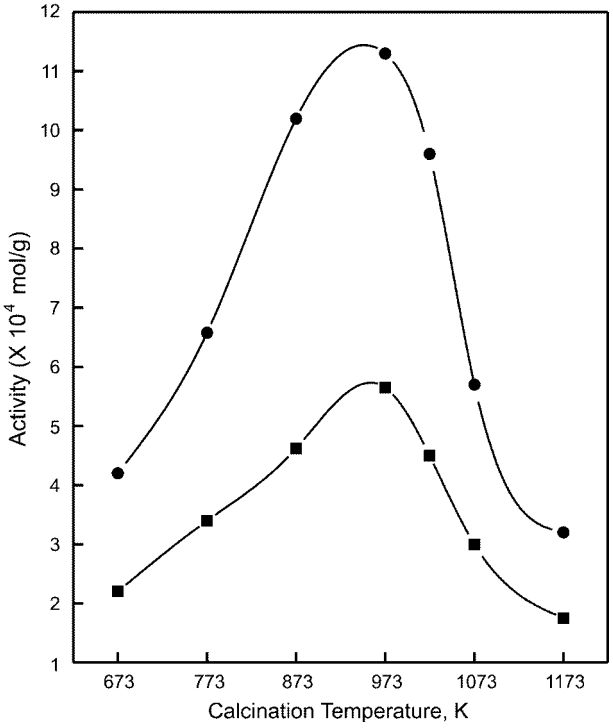

Fig. 12. Catalytic activity of $4V_2O_5$-$10WO_3/ZrO_2$ for 2-propanol dehydration as a function of calcination temperature. ●, 453 K; ■, 433 K.

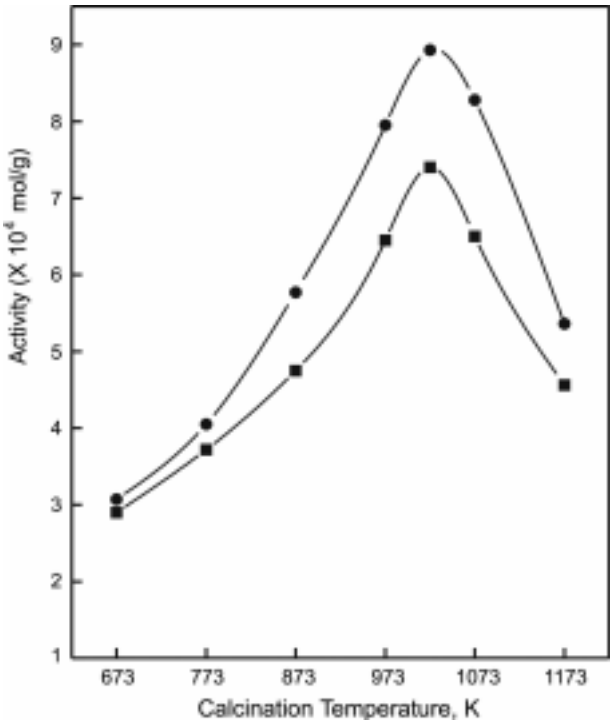

Fig. 13. Catalytic activity of $12V_2O_5$-$15WO_3/ZrO_2$ for cumene dealkylation as a function of calcination temperature. ●, 723 K; ■, 673 K.

ties for both reactions above 973-1,023 K can be probably attributed to the fact that the surface area and acidity above 973-1,023 K decrease with the calcination temperature [Sohn and Park, 2002].

CONCLUSIONS

On the basis of the results of FTIR, Raman and XRD, at low calcination temperature of 773 K vanadium oxide up to 12 wt% was well dispersed on the surface of zirconia. However, high V_2O_5 loading (equal to or above 18 wt%) on the surface of zirconia was well crystallized. The ZrV_2O_7 compound was formed through the reaction of V_2O_5 and ZrO_2 at 873 K and the compound decomposed into V_2O_5 and ZrO_2 at 1,073 K, which was observed in the spectra of FTIR and XRD. The W=O bands (1,012 cm^{-1}) due to wolframyl species strongly suggests that they interact with the zirconia via W-O-Zr bonds. It is suggested tat the increase of acidic sites and their acid strength may be attributable to electronic and structural interaction between vanadium oxide and tungsten oxide species on the ZrO_2 surface. The variations in catalytic activities for 2-propanol dehydration and cumene dealkylation are roughly correlated with the changes of acidity.

REFERENCES

Afanasiev, P., Geantet, C., Breysse, M., Coudurier, G. and Vedrine, J. C., "Influence of Preparation Method on the Acidity of $MoO_3(WO_3)/ZrO_2$ Catalysts," *J. Chem. Soc., Faraday Trans.*, **90**, 193 (1994).

Alemany, L. J., Lietti, L., Ferlazzo, N., Forzatti, P., Busca, G., Giamello, E. and Bregani, F., "Reactivity and Physicochemical Characterization of V_2O_5-WO_3/TiO_2 De-NO_x Catalysts," *J. Catal.*, **155**, 117 (1995).

Arata, K., "Solid Superacids," *Adv. Catal.*, **37**, 165 (1990).

Arco, M. del, Holgado, M. J., Martin, C. and Rives, V., "Reactivity of Vanadia with Silica, Alumina, and Titania Surfaces," *Langmuir*, **6**, 801 (1990).

Armor, J. N., "Environmental Catalysis," *Appl. Catal. B: Environmental*, **1**, 221 (1992).

Barton, D. G., Shtein, M., Wilson, R. D., Soled, S. L. and Iglesia, E., "Structural and Electronic Properties of Solid Acids Based on Tungsten Oxide Nanostructures," *J. Phys. Chem. B*, **103**, 630 (1999).

Bjorklund, R. B., Odenbrand, C. U. I., Brandin, J. G. M., Anderson, L. A. H. and Liedberg, B., "An Infrared and Electrical Conductance Study of V_2O_5/SiO_2-TiO_2 Catalysts Active for the Reduction of NO by NH_3," *J. Catal.*, **119**, 187 (1989).

Busca, G., Elmi, A. S. and Forzatti, P., "Mechanism of Selective Methanol Oxidation over Vanadium Oxide-Titanium Oxide Catalysts: A FT-IR and Flow Reactor Study," *J. Phys. Chem.*, **91**, 5263 (1987).

Cavani, F., Centi, G., Foresti, E. and Trifiro, F., "Surface Structure and Reactivity of Vanadium Oxide Supported on Titanium Dioxide," *J. Chem. Soc., Faraday Trans., 1*, **84**, 237 (1988).

Centi, G., Pinelli, D., Trifiro, F., Ghoussoub, D., Guelton, M. and Gengembre, L., "Surface Structure and Reactivity of V-Ti-O Catalysts Prepared by Solid-State Reaction," *J. Catal.*, **130**, 238 (1991).

Chan, S. S., Wachs, I. E. and Murrell, L. L., "Relative Raman Cross-Sections of Tungsten Oxides: [WO_3, $Al_2(WO_4)_3$ and WO_3/Al_2O_3]," *J. Catal.*, **90**, 150 (1984).

DeCanio, S. J., Sohn, J. R., Fritz, P. O. and Lunsford, J. H., "Acid Catalysis by Dealuminated Zeolite-Y," *J. Catal.*, **101**, 132 (1986).

Dines, T. J., Rochester, C. H. and Ward, A. M., "Raman Spectroscopic

Study of Titania-supported Vanadia Catalysts," *J. Chem. Soc. Faraday. Trans.*, **87**, 653 (1991).

Ebitani, K., Konishi, J. and Hattori, H., "Skeletal Isomerization of Hydrocarbons over Zirconia Oxide Promoted by Platinum and Sulfate Ion," *J. Catal*., **130**, 257 (1991).

Elmi, A. S., Tronoconi, E., Cristiani, C., Martin, J. P. G. and Forzatti, P., "Mechanism and Active Sites for Methanol Oxidation to Methyl Formate over Coprecipitated Vanadium-Titanium Oxide Catalysts," *Ind. Eng. Chem. Res*., **28**, 387(1989).

Engweiler, J., Harf, J. and Baiker, A., "WO_x/TiO_2 Catalysts Prepared by Grafting of Tungsten Alkoxides; Morphological Properties and Catalytic Behavior in the Selective Reduction of NO by NH_3," *J. Catal*., **159**, 259 (1996).

Gutierrez-Alejandre, A., Ramirez, J. and Busca, G., "A Vibrational and Spectroscopic Study of WO_3/TiO_2-Al_2O_3 Catalyst Precursors," *Langmuir*, **14**, 630 (1998).

Hatayama, F., Ohno, T., Maruoka, T. and Miyata, H., "Structure and Activity of Vanadium Oxide Layered on Titania (Anatase and Rutile)," *J. Chem. Soc., Faraday Trans*., **87**, 2629 (1991).

Highfield, J. G. and Moffat, J. B., "Characterization of 12-Tungstophosphoric Acid and Related Salts Using Photocoustic Spectroscopy in the Infrared Region," *J. Catal*., **88**, 177 (1984).

Hino, M. and Arata, K., "Synthesis of Solid Superacid of Tungsten Oxide Supported on Zirconia and its Catalytic Action for Reactions of Butane and Pentane," *J. Chem. Soc. Chem. Commun*., 1259 (1987).

Hsu, C. Y., Heimbuch, C. R., Armes, C. T. and Gates, B. C., "A Highly Active Solid Superacid Catalyst for n-Butane Isomerization: a Sulfated Oxide Containing Iron, Manganese and Zirconium," *J. Chem. Soc. Chem. Commun*., 1645 (1992).

Iglesia, E., Soled, S. L. and Kramer, G. M., "Isomerization of Alkanes on Sulfated Zirconia: Promoted by Pt and by Ad Amantyl Hydride Transfer Species," *J. Catal*., **144**, 238 (1993).

Kim, D. S., Ostromecki, M. and Wachs, I. E., "Surface Structures of Supported Tungsten Oxide Catalysts under Dehydrated Coditions," *J. Mol. Catal. A: Chemical*, **106**, 93 (1996).

Kustov, L. M., Kazansky, V. B., Figueras, F. and Tichit, D., "Investigation of the Acidic Properties of ZrO_2 Modified by SO_4^{2-} Anions," *J. Catal*., **150**, 143 (1994).

Lakshmi, L. J., Ju, Z. and Alyea, E., "Synthesis, Characterization and Activity Studies of Vanadia Supported on Zirconia and Phosphorus-Modified Zirconia," *Langmuir*, **15**, 3521 (1999).

Larrubia, M. A., Ramis, G. and Busca, G., "An FT-IR Study of the Adsorption of urea and ammonia over V_2O_5-MoO_3-TiO_2 SCR Catalysts," *Appl. Catal. B:Environmental*, **27**, L145 (2000).

Larsen, G., Lotero, E. and Parra, R. D., "Tungsta and Platinum-Tungsta Supported on Zirconia Catalysts for Alkane Isomerization," in Proc. 11th Int. Congr. Catal., 543 (1996).

Larsen, G., Lotero, E., Petkovic, L. M. and Shobe, D. S., "Alcohol Dehydration Reactions over Tungstated Zirconia Catalysts," *J. Catal*., **169**, 67 (1997).

Lee, J. K. and Rhee, H. K., "Effect of Metal/Acid Balance in Pt-Loaded Large Pore eolites on the Hydroisomerization of n-Heptane," *Korean J. Chem. Eng*., **14**, 1251 (1997).

Mercera, P. D. L., Van Ommen, J. G., Doeburg, E. B. M., Burggraaf, A. J. and Ross, J. R. H., "Zirconia as a Support for Catalysts Evolution of the Texture and Structure on Calcination in Air," *Appl. Catal*., **57**, 127 (1990).

Miyata, H., Kohno, M., Ono, T., Ohno, T. and Hatayama, F., "Structure of Vanadium Oxides on ZrO_2 and the Oxidation of Butene," *J. Chem. Soc., Faraday Trans. 1*, **85**, 3663 (1989).

Miyata, H., Fujii, K., Ono, T., Kubokawa, Y., Ohno, T. and Hatayama, F., "Fourier-transform Infrared Investigation of Structures of Vanadium Oxide on Various Supports," *J. Chem. Soc., Faraday Trans*., **83**, 675 (1987).

Mori, K., Miyamoto, A. and Murakami, Y., "Activity and Selectivity in Toluene Oxidation on Well Characterized Vanadium Oxide Catalysts," *J. Chem. Soc., Faraday Trans. 1*, **83**, 3303 (1987).

Paganini, M. C., Dall'Acqua, L., Giamello, E., Lietti, L., Forzatti, P. and Busca, G., "An EPR Study of the Surface Chemistry of the V_2O_5-WO_3/TiO_2 Catalyst: Redox Behaviour and state of V(IV)," *J. Catal*., **166**, 195 (1997).

Park, E. H., Lee, M. H. and Sohn, J. R., "Solid-State ^{51}V NMR and Infrared Spectroscopic Study of Vanadium Oxide Supported on TiO_2-ZrO_2," *Bull. Korea Chem. Soc*., **21**, 913 (2000).

Ramis, G., Cristiani, C., Forzatti, P. and Busca, G., "On the Consistency of Data Obtained from Different Techniques Concerning the Surface Structure of Vanadia-Titania Catalysts," *J. Catal*., **124**, 574 (1990).

Roozeboom, F., Mittelmelijer-Hazeleger, M. C., Moulijn, J. A., Medema, J., de Beer, U. H. J. and Gelling, P. J., "Vanadium Oxide Monolayer Catalysts. 3. A Raman Spectroscopic and Temperature-Programmed Reduction Study of Monolayer and Crystal-type Vanadia on Various Supports," *J. Phys. Chem*., **84**, 2783 (1980).

Sachtler, W. M. H., "The Mechanism of the Catalytic Oxidation of Some Organic Molecules," *Catal. Rev.*, **4**, 27 (1971).

Salvati, L., Makovsky, L. E., Stencel, J. M., Brown, F. R. and Hercules, D. M., "Surface Spectroscopic Study of Tungsten-Alumina Catalysts Using X-ray Photoelectron, Ion Scattering, and Raman Spectroscopies," *J. Phys. Chem*., **85**, 3700 (1981).

Scharf, U., Schraml Marth, M., Wokaun, A. and Baiker, A., "Comparison of Grafted Vanadia Species on ZrO_2, TiO_2, SiO_2 and TiO_2/SiO_2 Mixed Oxides," *J. Chem. Soc., Faraday Trans.*, **87**, 3299 (1991).

Scheithauer, M., Grasselli, R. K. and Knözinger, H., "Genesis and Structure of WO_x/ZrO_2 Solid Acid Catalysts," *Langmuir*, **14**, 3019 (1998).

Schild, C. H., Wokaun, A., Köppel, R. A. and Baiker, A., "XRD and Raman Identification of the Zirconia Modifications in Copper/Zirconia and Palladium/Zirconia Catalysts Prepared from Amorphous Precursors," *J. Catal*., **130**, 657 (1991).

Sohn, J. R. and Bae, J. H., "Characterization of Tungsten Oxide Supported on TiO_2 and Activity for Acid Catalysis," *Korean J. Chem. Eng*., **17**, 86 (2000).

Sohn, J. R., Cho, S. G., Pae, Y. I. and Hayashi, S., "Characterization of Vanadium Oxide-Zirconia Catalyst," *J. Catal*., **159**, 170 (1996).

Sohn, J. R., Kim, T. G., Kwon, T. D. and Park, E. H., "Characterization of Titanium Sulfate Supported on Zirconia and Activity for Acid Catalysis," *Langmuir*, **18**, 1666 (2002).

Sohn, J. R. and Park, M. Y., "Characterization of Zirconia-Supported Tungsten Oxide Catalyst," *Langmuir*, **14**, 6140 (1998).

Sohn, J. R., Park, M. Y. and Pae, Y. I., "Characterization by Solid-State ^{51}V NMR and X-ray Diffraction of Vanadium Oxide Supported on ZrO_2," *Bull. Korean Chem. Soc*., **17**, 274 (1996).

Sohn, J. R. and Park, W. C., "Characterization of Nickel Sulfate Supported on γ-Al_2O_3 and its Relationship to Acidic Properties," *Korean J. Chem. Eng*., **19**, in press (2002).

Toda, Y., Ohno, T., Hatayama, F. and Miyata, H., "Effect of WO_3 in mixed V_2O_5-WO_3/ZrO_2 Catalysts on Their Surface Structures and Decomposition of Propanol-2-ol," *Phys. Chem. Chem. Phys.*, **1**, 1615 (1999).

Vaudagna, S. R., Canavese, S. A., Comelli, R. A. and Figoli, N. S., "Platinum Supported WO_x-ZrO_2: Effect of Calcination Temperature and Tungsten Loading," *Appl. Catal. A: General*, **168**, 93 (1998).

Vaudagna, S. R., Comelli, R. A., Canavese, S. A. and Figoli, N. S., "SO_4^{2-}-ZrO_2 and Pt/SO_4^{2-}-ZrO_2: Activity and Stability during n-Hexane Isomerization," *J. Catal.*, **169**, 389 (1997).

Vuurman, M. A., Wachs, I. E. and Hirt, A. M., "Structural Determination of Supported V_2O_5-WO_3/TiO_2 Catalysts by in Situ Raman Spectroscopy and X-ray Photoelectron Spectroscopy," *J. Phys. Chem.*, **95**, 9928 (1991).

Wan, K. T., Khouw, C. B. and Davis, M. E., "Studies on the Catalytic Activity of Zirconia Promoted with Sulfate, Iron, and Manganese," *J. Catal.*, **158**, 311 (1996).

Ward, D. A. and Ko, E. I., "One-step Synthesis and Characterization of Zirconia-Sulfate Aerogels as Solid Superacids," *J. Catal.*, **150**, 18 (1994).

Yuan, X.-D., Park, J.-N, Wang, J., Lee, C. W. and Park, S.-E., "Alkylation of Benzene with 1-Dodecane over USY Zeolite Catalyst: Effect of Pretreatment and Reaction Conditions," *Korean J. Chem. Eng.*, **19**, 607 (2002).

Zhao, B., Xu, X., Gao, J., Fu, Q. and Tang, Y., "Structure Characterization of WO_3/ZrO_2 Catalysts by Raman Spectroscopy," *J. Raman Spectrosc.*, **27**, 549 (1996).